Journal of Electroanalytical Chemistry 638 (2010) 262–268

Contents lists available at ScienceDirect

Journal of Electroanalytical Chemistry

journal homepage: www.elsevier.com/locate/jelechem

Self-assembled multilayers of polyethylenimine, DNA and gold nanoparticles. A study of electron transfer reaction

Nancy F. Ferreyra [a,*], Soledad Bollo [b], Gustavo A. Rivas [a]

[a] INFIQC, Departamento de Fisicoquímica, Facultad de Ciencias Químicas, Universidad Nacional de Córdoba, 5000 Córdoba, Argentina
[b] Laboratorio de Bioelectroquímica, Facultad de Ciencias Químicas y Farmacéuticas, Universidad de Chile, P.O. Box 233, Santiago, Chile

ARTICLE INFO

Article history:
Received 19 October 2009
Accepted 2 November 2009
Available online 10 November 2009

Keywords:
Scanning Electrochemical Microscopy
Polyethylenimine
DNA
Self-assembled multilayers
Gold nanoparticles

ABSTRACT

The present manuscript describes studies of the electron transfer kinetics at gold electrodes modified by electrostatic self-assemblies of polyethylenimine (PEI), DNA and gold nanoparticles (NP) by Scanning Electrochemical Microscopy (SECM). Two redox mediators of similar structure, ferrocenemethanol (FcOH), and ferrocenecarboxylic acid (FcCOOH) were used to evaluate the effect of the electrode modification on the electron transfer process. For both redox probes, the observed electrochemical behavior was dependent of the charge of the external layer of the self-assembled structure. The corresponding apparent heterogeneous rate constant, k^0, was determined. The effect of NP adsorption was also evaluated. Independently of the mediator used, an increase of the k^0 was observed when NPs were incorporated, and the surfaces presented a conductive behavior similar to the bare gold electrode. SECM images using FcOH as redox mediator were also recorded. Variations in the normalized currents permitted to evaluate differences of the surface electroactivity due to the polymers and/or nanoparticles adsorption.

1. Introduction

Electrostatic layer-by-layer assembly is a highly attractive approach for the construction of functional multilayer architectures at electrodes surfaces, particularly for sensing purposes [1]. Self-assembled process traditionally involves the alternate contact with polyelectrolyte pairs (i.e., a polyanion and a polycation) [2] to form polyelectrolyte (PE) multilayers (PEM). In these systems, adsorption is typically driven via electrostatic interactions with a charged substrate. Adsorption results in charge overcompensation, which then facilitates the subsequent adsorption of another, oppositely charged PE. Using this easy-of-operation technique is possible to control the surface charge and the thickness of the film in a quite simple way [2]. Proteins, enzymes, DNA, polymers and nanoparticles of different materials have been incorporated in self-assembled multilayers [3]. The combination of nanomaterials and biomolecules is of great interest in the field of electroanalysis. Nanoparticles (NP) are important in the immobilization of biomolecules due to their large specific surface area, excellent biocompatibility and good conductivity. In addition, metal nanoparticles contribute to facilitate the electron transfer to redox molecules, acting as tiny conduction centers [4]. NP provide a general route for the development of biosensors as they enable immobilization of a variety of biomolecules. Recently, nanostructured films fusing the properties of metallic nanoparticles and DNA have been reported [5,6]. The combination of the recognition capability of DNA with the particular properties of the nanoparticles makes these platforms very attractive for the development of biosensors. Understanding structure-properties relationships of NP-modified electrodes is a key step in their effective application in electrochemistry.

Several techniques have been used to characterize the multilayers structure. Among them, the electrochemical ones allow evaluating the electron transfer kinetics to redox probes, which are connected to the transport properties across the PEM. Scanning Electrochemical Microscopy (SECM) makes possible both, to study the electron transfer (ET) process and to distinguish between regions of different conductivity or electrochemical activity with high spatial resolution [7–12]. Some few examples of SECM application to study the effect of NP in the electrochemical reactivity of self-assembled structures have been reported [13–17]. In a recent review, Merkoçi et al. [18] have described the advantages of the SECM to investigate intrinsic electrochemical properties and also catalytic features of NP. On the other hand, Bard and coworkers employing ultramicroelectrodes have studied the electrocatalytic activity of Pt nanoparticles modified with alkane thiols [19,20].

In this work we propose the use of SECM to study charge transfer processes of redox probes across self-assembled multilayers of

* Corresponding author. Tel.: +54 351 4334169/80x121; fax: +54 351 4334188.
E-mail address: ferreyra@fcq.unc.edu.ar (N.F. Ferreyra).

0022-0728/$ - see front matter © 2009 Elsevier B.V. All rights reserved.
doi:10.1016/j.jelechem.2009.11.009

polyethylenimine (PEI), dsDNA and gold nanoparticles (NP). The goal is to evaluate the effect of the different self-assembled layers, and, particularly, the changes observed after the adsorption of nanoparticles on the electrochemical activity at the electrode surface.

2. Experimental part

2.1. Reagents

Polyethylenimine (PEI) 50% w/v (Catalog number P-3143), gold nanoparticles (NP) citrate stabilized of 10 nm nominal diameter (Catalog number G-1527) and double stranded calf thymus DNA (dsDNA) (activated and lyophilized, catalog number D4522) were from Sigma. DNA stock solutions (1000 ppm) were prepared in Tris–EDTA (TE) buffer (1× concentrate, 20 mM Tris–HCl, 1 mM EDTA, pH 8.0), while the dilutions were made using a 0.10 M phosphate buffer solution pH 7.50. DNA concentration was determined by UV–Vis spectroscopy. 3-mercapto-1-propanesulfonic acid (MPS), ferrocenemethanol (FcOH) and ferrocenecarboxylic acid (FcCOOH) were from Aldrich. Other chemicals were reagent grade and used without further purification. All solutions were prepared with ultra-pure water (18 MΩ cm) from a Millipore MilliQ system.

2.2. Equipment

Cyclic Voltammetry and Scanning Electrochemical Microscopy were performed with a CHI 900 (CH Instruments Inc., USA). Gold disk electrodes (Au) of 3 mm diameter (CHI 101) were used as substrate. Chronoamperometric experiments to determine the redox mediator diffusion coefficient were performed using a CHI 400 (CH Instruments Inc., USA) and a glassy carbon of 0.070 cm^2 geometric area (CHI 104) as working electrode. In all the experiments a platinum wire and Ag/AgCl, 3 M NaCl (BAS, Model RE-5B) were used as counter and reference electrodes, respectively. A homemade carbon fiber electrode of ca. 10 μm diameter served as SECM ultramicroelectrode (UME) (RG = 10). It was prepared as follows: a 10 μm carbon fiber was washed with acetone, dried, and placed into a 10 cm long, 1 mm i.d. Pyrex tube sealed at one end. The oxygen was removed by introducing argon through the open end of the tube, in order to avoid the carbonization of the fiber. The sealed end of the tube was heated with a helix heating coil to seal the glass around the fiber. This extreme was polished with sandpaper until the carbon fiber cross sections was exposed, and then with 0.05 μm alumina paste (Buehler, Ltd., Lake Bluff, IL). The electrical contact with a Cu wire was made of silver paint. The glass-wall surrounding carbon fiber was conically sharpened with sandpaper until the diameter of the flat glass section surrounding the carbon fiber was ~100 μm. The evaluation was performed by optical microscopy. Finally, the tip was polished with alumina before each experiment. The tip radius was verified by cyclic voltammetry.

2.3. Modification of the working electrode

The cleaning procedure of gold electrodes included polishing with 0.05 μm alumina for 6 min, careful sonication in deionized water for 5 min, and immersion in "Piranha" solution (1:3 v/v H_2O_2/98% H_2SO_4) for 10 min, followed by a rinsing step with ultra-pure water. Caution: "Piranha" solution is very corrosive and must be handled with care. The clean surfaces were stabilized by cycling the potential between 0.200 V and 1.650 V at 10 V s^{-1} in a 0.50 M sulfuric acid solution until obtaining a reproducible response. Before each experiment a cyclic voltammogram at 0.100 V s^{-1} in the same supporting electrolyte solution was performed to check the surface conditions.

The adsorption of MPS was performed by soaking the electrode for 30 min in a 2.00×10^{-2} M MPS prepared in 1.6×10^{-3} M sulfuric acid solution, followed by a careful rinsing with deionized water.

The multilayer system was obtained by alternate immersions in PEI and dsDNA. PEI adsorption was performed from a 2.0 mg mL^{-1} aqueous solution for 20 min, while dsDNA was adsorbed from 100 ppm solutions prepared in 0.10 M phosphate buffer pH 7.50 for 60 min. After each immersion step, the electrode was copiously rinsed with phosphate buffer. The resulting electrodes are indicated as Au/MPS/PEI-dsDNA.

To evaluate the effect of gold nanoparticles, we adsorbed bilayers of PEI-NP alternatively with PEI-dsDNA bilayers. The adsorption of gold NP was obtained by immersion of the electrodes in a NP solution for 60 min. After that, the surface was copiously rinsed with buffer solution. The resulting electrodes are indicated as Au/MPS/PEI-NP/PEI-dsDNA.

To evaluate the effect of the NP adsorption time on the electrochemical response of the redox probes, NP were adsorbed 15, 30, 60 or 120 min on the top of Au/MPS/PEI electrode.

2.4. SECM

The feedback mode was selected as operation mode of SECM and it is essentially based on the measurement of the current produced at the ultramicroelectrode (UME), i_T, when it is brought close to the substrate in the presence of a redox mediator [21–22]. Far from the substrate the steady-state current of the UME is $i_{T,\infty} = 4naFDC$, where n is the number of electrons transferred per redox event, F the Faraday constant, D the diffusion coefficient of the electroactive specie and "a" is the tip radius. In the diffusion-controlled positive feedback case, $i_T > i_{T,\infty}$, indicating that the substrate acts as a conductive surface producing an additional flux of the redox mediator at the UME. On the contrary, in the negative feedback case, $i_T < i_{T,\infty}$, meaning that the substrate acts as an electrical insulator hinders the flux of the redox mediator to the surface of the UME [23].

2.4.1. Determination of k^0

The heterogeneous rate constants k^0 for the electron transfer (ET) reaction were obtained by fitting the experimental current vs. distance curve (i_T–d), to the theoretical values [24]. Scheme 1 shows a diagram of the SECM experimental setup employed.

2.4.2. SECM Images

SECM feedback mode was selected to obtain images of each modified surface using a 5.0×10^{-4} M FcOH solution. The UME and the substrate potentials were held at 0.500 V and 0.000 V, respectively, allowing the feedback takes place between both electrodes. Part of the gold electrode (no more than 1/3 of its surface) was kept without modification; the UME was approached to this unmodified section at a scan rate of 0.5 μm s^{-1} and automatically stopped when the current reached 1.25 times $i_{T,\infty}$. According to the theoretical curve that describes the dependence of i_T vs. distance between UME and substrate (d), a value equal to 1.25 $i_{T,\infty}$ corresponds to a separation of ~10 μm for an UME of 5 μm and RG ~ 10. RG is the ratio of the radius of the insulating sheath around the electrode and the carbon fiber [21].

Once the approach curve was done, the UME was moved in the x direction to make sure it was over the film, and then a series of constant height images were recorded in a 100 μm × 100 μm area at 1 μm s^{-1} UME scan rate. The results are presented in a dimensionless form normalizing the experimental feedback current, i_T, by the steady-state current $i_{T,\infty}$.

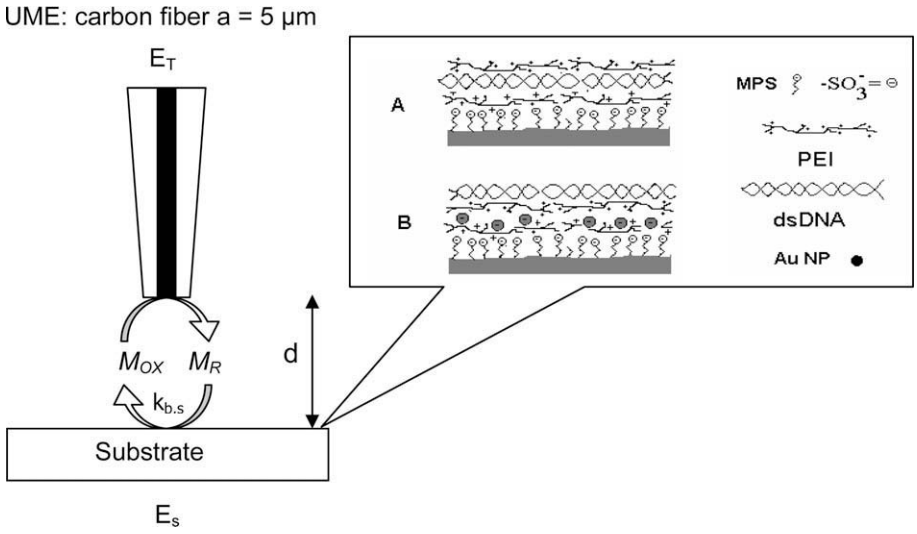

Scheme 1. Diagram of the SECM experimental setup and the modified electrodes without (A) and with gold nanoparticles adsorbed (B).

3. Results and discussion

3.1. Electrochemical activity at the PEM modified surface

To evaluate the influence of the external layer of the PEM on the electrochemical activity at the surface, two redox labels were used, FcOH and FcCOOH. The results obtained at gold electrodes modified with MPS, PEI, dsDNA and NP, were compared. Fig. 1 presents the approach curves obtained at: (a) Au, (b) Au/MPS, (c) Au/MPS/PEI, and d) Au/MPS/PEI-dsADN for FcOH, (Fig. 1A), and FcCOOH, (Fig. 1B), while applying $E_T = 0.500$ V and $E_S = 0.000$. Under this condition, at both electrodes a diffusion-controlled process is promoted. A rather fast regeneration of FcOH is observed at bare gold (a), and Au/MPS (b), while at Au/MPS/PEI (c) and Au/MPS/PEI-dsADN (d) the electron transfer is slower, particularly when the external layer is the polycation PEI, (curve c). These results are consistent with that obtained by cyclic voltammetry; Table 1 shows the values of ΔE_p of the different modified electrodes from voltammograms recorded at 0.100 V s^{-1}. Labbé et al. [25], have demonstrated that MPS monolayer is a rather open structure whit a 60% of the coverage reported for a densely packed thiol monolayer, that constitutes a kinetic barrier toward the permeation of FcOH because of its high hydrophobicity. As a consequence, the electron transfer of this redox probe mainly occurs by electron tunneling through the MPS layer, since the contribution of MPS-free pinholes and defects is low. Accordingly, the cyclic voltammogram of FcOH at 0.100 V s^{-1} is only slightly perturbed by the presence of MPS. Our results are in good agreement with this information. On the other hand, the adsorption of PEI and dsDNA at the top of MPS constitutes a barrier that avoids a closer approximation of FcOH to the electrode surface producing an increase in ΔE_p value, particularly when the external layer is PEI, and less conductive approach curves.

Regarding the behavior of FcCOOH (Fig. 1B), a conductive behavior is observed at bare electrode while the ET is partially blocked after the adsorption of MPS, PEI and dsDNA. The electrostatic repulsion between the negatively charged MPS and the anionic probe (at the pH employed) could be the reason for this SECM

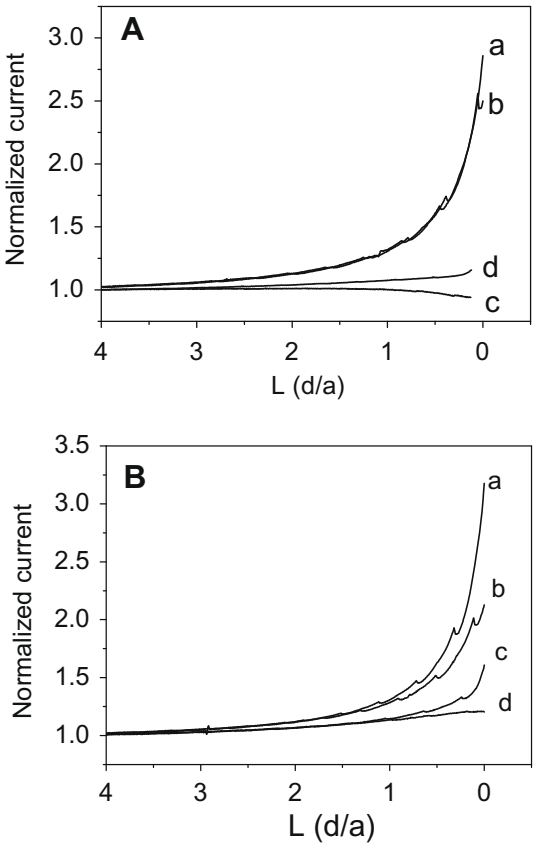

Fig. 1. Normalized current–distance curves for the UME approaching to: (a) Au, (b) Au/MPS, (c) Au/MPS/PEI, and (d) Au/MPS/PEI-dsDNA in (A) 5.0×10^{-4} M FcOH, and (B) 5.0×10^{-4} M FcCCOH. $E_T = 0.500$ V and $E_s = 0.000$ V. Supporting electrolyte 0.10 M phosphate buffer pH 7.5.

Table 1
Variation of peak potential separation as function of the electrode modification.

Surface	FcOH ΔE_p (V)	fccOOH ΔE_p (V)
Au	0.071	0.069
Au/MPS	0.097	0.155
Au/MPS/PEI	0.350	0.210
Au/MPS/PEI-dsDNA	0.145	0.245
Au/MPS/PEI-NP 15 min ads.	0.061	0.073
Au/MPS/PEI-NP 30 min ads.	0.061	0.067
Au/MPS/PEI-NP 60 min ads.	0.062	0.067
Au/MPS/PEI-NP 120 min ads.	0.064	0.067

behavior and the increase observed by cyclic voltammetry in the ΔE_p value.

These results evidence a selective response of the surface depending on the redox mediator used, since a modification on the electroactivity is observed when changing the mediator.

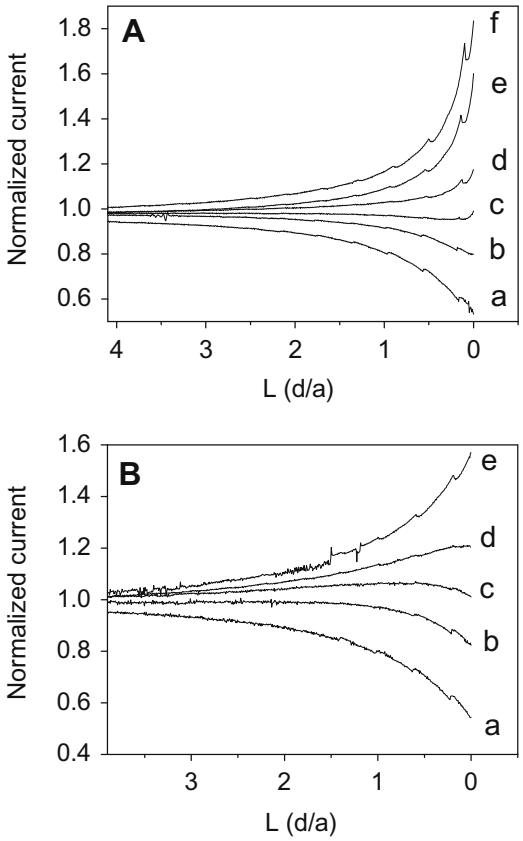

Fig. 2. Normalized current–distance curves for the UME approaching to Au/MPS/(PEI-dsDNA)$_1$ in (A) 5,0 $\times$ 10^{-4} M FcOH, E_T = 0.500 V and E_s: (a) 0.150 V, (b) 0.100 V, (c) 0.050 V, (d) 0.00 V (e) −0.050 V and (f) −0.100 V; and (B) 5.0 $\times$ 10^{-4} M fccOOH, E_T = 0.500 V and E_s: (a) 0.200 V, (b) 0.100 V, (c) 0.050 V (d) 0.000 V and (e) −0.050 V. Supporting electrolyte 0.10 M phosphate buffer pH 7.5.

3.2. Electron transfer behavior at Au/MPS/PEI-dsDNA modified electrode

To get a better inside of the electrochemical response of FcOH and FcCOOH we evaluate the effect of the substrate overpotential at Au/MPS/PEI-dsDNA from normalized current vs. distance curves. The UME, at a constant potential, E_T, was approached to the modified surface kept at different potential, E_S. Fig. 2A shows the curves corresponding to FcOH at E_T 0.500 V and E_s between 0.150 V (a) and –0.100 (f), while Fig. 2B displays the approach curves obtained using FcCOOH at E_T 0.500 V and E_S between 0.200 V (a) and −0.050 (e). On the top of this surface, both redox mediators present a quasireversible electrochemical behavior being ΔE_p = 0.145 V and E_{pc} = 0.150 V for FcOH and ΔE_p = 0.245 V and E_{pc} = 0.205 V for FcCOOH. Therefore, a change in the substrate overpotential, η, will influence the rate constant for the reduction of the mediators at the substrate ($k_{b,s}$) and the resulting feedback current. When the energy applied to the substrate is not enough, E_S close to $E_{pc,}$ e.g., 0.150 V for FcOH or 0.200 V for FcCOOH, (curves a in Figs. 2A and B, respectively), the approach curve obtained is close to the theoretical one for pure negative feedback. As the substrate potential becomes more negative, a positive measurable feedback is

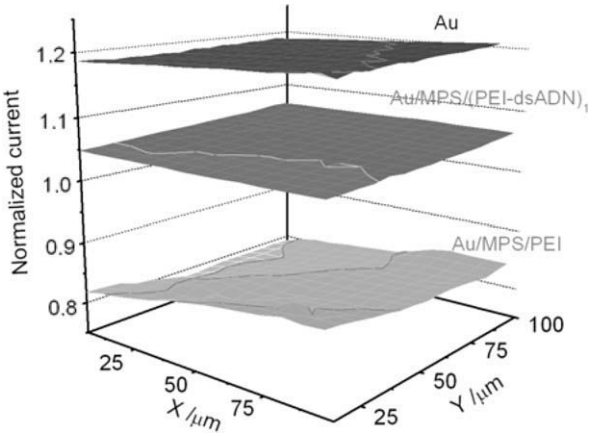

Fig. 4. Surface-plot images of Au, Au/MPS/PEI-dsDNA, and Au/MPS/PEI in 5.0 $\times$ 10^{-4} M FcOH, E_T = 0.500 V and E_s = 0.000 V. Image parameters: 100 μm $\times$ 100 μm at 1 μm s^{-1} UME scan rate. Supporting electrolyte 0.10 M phosphate buffer pH 7.5.

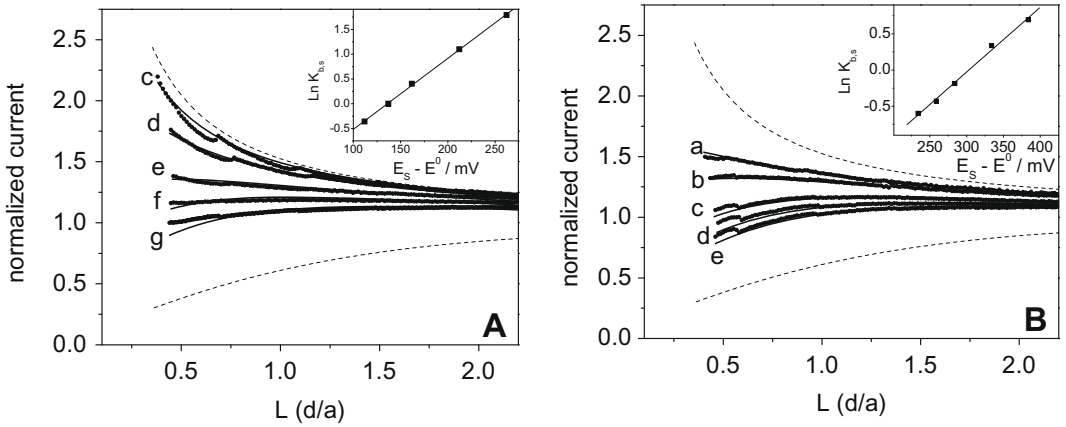

Fig. 3. Experimental (dotted) and simulated (solid lines) approach curves for (A) Au/MPS, (B) Au/MPS/PEI-dsDNA using 5.0 $\times$ 10^{-4} M fccOOH, E_T = 0.500 V and E_s: (a) −0.050 V, (b) 0.000 V, (c) 0.050 V, (d) 0.075 V, (e) 0.100 V, (f) 0.150 V (g) 0.200 V. The upper and the bottom dashed lines represent the theoretical positive and negative feedback curves, respectively. Insets show the corresponding plots for the determination of k^0. The small deviation in the experimental data at d/a ∼0.6 is an artifact due to the clamping action of the coarse piezo positioners.

observed, indicating a fast regeneration of FcOH and FcCOOH at Au/MPS/PEI-dsADN. On the other hand, comparing the approach curves for both redox mediatos at the same substrate potential, e.g. for E_s = 0.000 V (curve d for FcCOOH and curve d for FcOH), it is clear that FcCOOH presents lower feedback current than FcOH. This effect could be related to the electrostatic repulsion between the charges of the supramolecular architecture ended in dsDNA and the carboxylate groups of the mediator at the solution pH.

3.3. Determination of k^0 at the modified electrode

A quantitative analysis of the ET rate variation at the modified surfaces was also done. The heterogeneous rate constants k^0 for the ET reaction were obtained by fitting the experimental current vs. distance curve (i_T–d) to the theoretical values to obtain the dimensionless kinetic parameter $K_{b,s}$, ($K_{b,s}$ = a $k_{b,s}$/D) [26,27]. For the final calculation it was necessary to determinate the diffusion coefficient of each compound in the reaction medium. For that purpose, chronoamperometric measurements were performed with 5.0×10^{-4} M solutions of redox mediator solutions in a 0.10 M phosphate buffer solution pH 7.50. The diffusion coefficient values obtained were: (8.0 ± 0.1) 10^{-6} cm^2 s^{-1} and (9.2 ± 0.2) 10^{-6} cm^2 s^{-1} for FcOH and FcCOOH, respectively. These values are in good agreement with previous reports [28–30].

Fig. 3 shows the experimental (dotted lines) and theoretical (solid lines) approach curves using FcCOOH as redox mediator at E_T = 0.500 V and different substrate potentials. The insets show the plots of ln $K_{b,s}$ vs. the overpotential applied to the surface. On the gold bare electrode, a complete conductor behavior is observed (ΔE_p = 0.070 V) (data not shown), while when the outer layer is MPS (Fig. 3A), the calculated k^0 value is $(2.64 \pm 0.08) \times 10^{-3}$ cms^{-1}. The repulsive interaction between MPS sulfonate and carboxylate groups hinders the process and produces a decrease of k^0. When dsDNA is adsorbed on the top of the structure, k^0 decreases up to $(1.1 \pm 0.5) \times 10^{-3}$ cms^{-1} probably due to the repulsive interaction of the negatively charged polyelectrolyte located in the outer layer

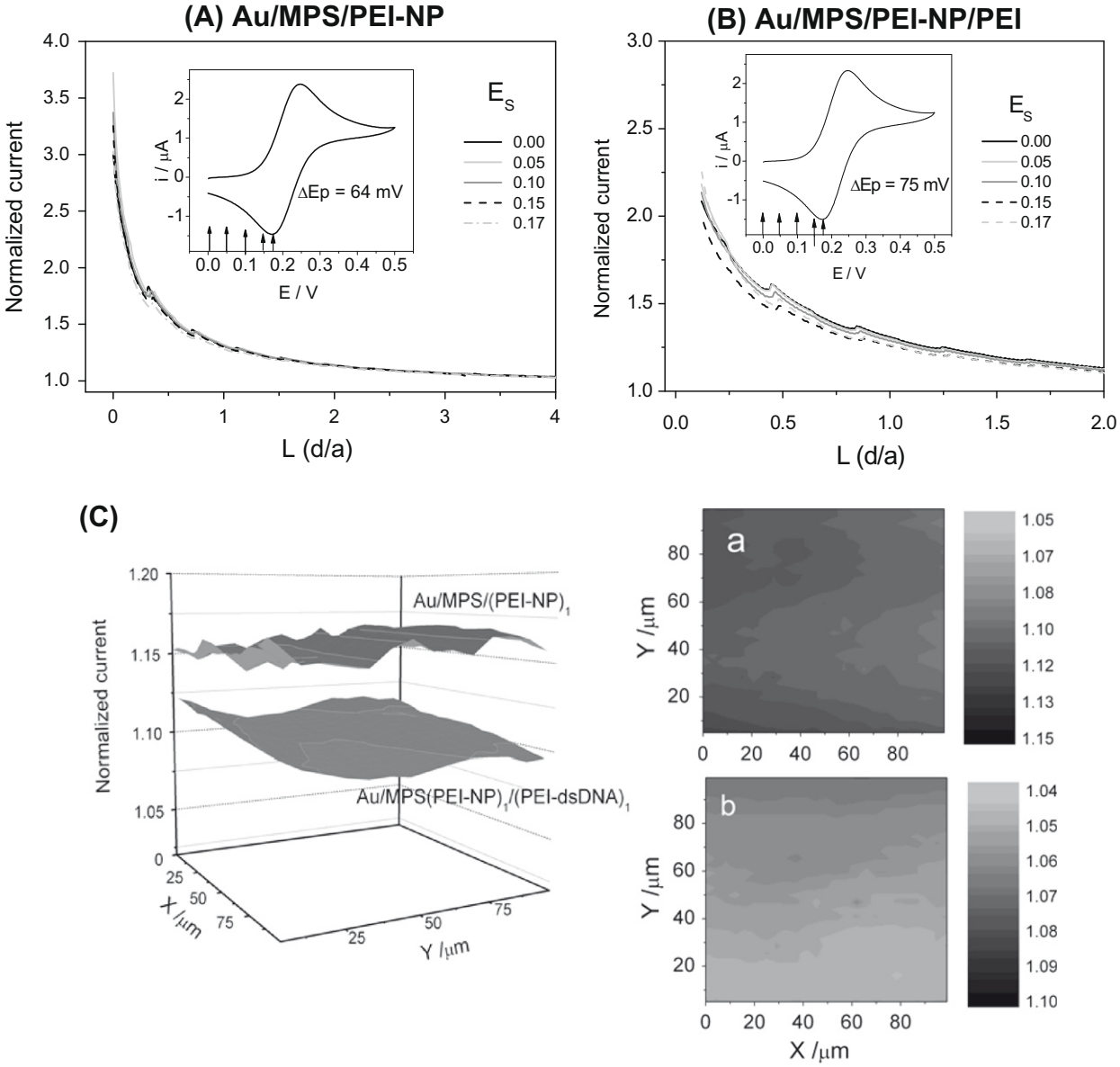

Fig. 5. Normalized current–distance curves for the UME approaching to: (A) Au/MPS/PEI-NP and (B) Au/MPS/PEI-NP/PEI with 60 min of NP adsorption time in 5.0×10^{-4} M FcOH, E_T = 0.500 V and E_s: 0.000 V, 0.050 V, 0.100 V, 0.150 V, and 0.170 V. Inset shows the CVs of the redox mediator at 0.100 V s^{-1}. The arrows indicates E_S applied. (C) Surface-plot images and contour images corresponding to (a) Au/MPS/PEI-NP and (b) Au/MPS/PEI-NP/PEI-dsDNA. Experimental conditions as Fig. 4.

with the carboxylate groups of FcCOOH. Taking into account the k^0 value determined from SECM, cyclic voltammogram at 0.100 V s^{-1} were simulated using software DIGISIM® 2.1CV simulator for Windows and a value of ΔE_p = 0.145 V and 0.215 V were obtained for AU/MPS and Au/MPS/PEI-dsDNA (not shown). The difference between calculated and experimental results is probably due to a more complex behavior than the one assumed in this paper. In this sense Amatore and coworkers [31] have proposed a theoretical analysis to treat cyclic voltammograms at a partially covered electrode with microscopic defect by a CEC mechanism instead of a simple E mechanism.

Similar experiments were performed with FcOH, (not shown). The results demonstrated a conductive behavior at bare gold electrode. At Au/MPS the ET rate becomes quasireversible, and a k^0 value of $(4.0 \pm 0.1) \times 10^{-2}$ cms^{-1} was determined. After the adsorption of the polycation PEI, the ET to the ferricinium cation is constrained by the electrostatic repulsion between the positively charged PEI and the oxidized mediator, and the response become slower. The k^0 value obtained for Au/MPS/PEI-dsDNA was $(2.4 \pm 0.4) \times 10^{-3}$ cm s^{-1} (ΔE_p = 0.145 V). In this case the simulated voltammogram presented a ΔE_p = 0.146 V.

Surface-plot images of the modified electrodes were also performed, we selected FcOH as redox mediator because it would allow differentiate electrochemical reactivity of the modified surfaces. The images were scanned at a UME-substrate distance of ~10 μm with a E_T = 0.500 V and a E_s = 0.000 V which ensure the maximum diffusion-controlled process at both, the UME and the gold modified electrodes. Fig. 4 shows the SECM surface-plot images, presented as normalized current of Au, Au/MPS/PEI surfaces, and Au/MPS/PEI-dsADN. At bare gold electrode, a typical substrate conductive behavior is observed, with current close to 1.20 times the steady-state value and a regular topography. At Au/MPS/PEI surface, the normalized current decreases from ~1.20 to ~0.80, in agreement with the behavior observed in the approach curves (Fig. 1A, curve c) confirming that PEI hinders the electrochemical response of ferricinium cation and consequently the diffusion-controlled feedback. On the other hand, when dsDNA is present in the outer layer of the surface an increase in the normalized current values is observed, being 1.05 times the steady-state current. The normalized currents of the surfaces are consistent with the k^0 values informed previously using FcOH. In all cases, homogeneous surfaces were obtained, indicating that the modifications did not produce significant changes in the electrode topography. As the literature report that a bilayer of PEI-dsDNA has a thickness of 4.5 nm [32], the adsorption of PEI-dsDNA produces a variation in the UME-surface distance that corresponds just to 2.3% of i_T value, therefore the differences observed in the normalized current can be associated to modification in ET of FcOH at the substrate and not to a topographic effect.

3.4. Influence of gold nanoparticles adsorbed at the PEM on the electrochemical behavior of the redox mediators

To evaluate the effect of the adsorption of gold nanoparticles at the PEM we compare the response obtained at Au/MPS/PEI-NP and Au/MPS/PEI-NP/PEI electrodes (Fig. 5A and B, respectively), employing 60 min of NP adsorption and FcOH as redox mediator. A series of approach curves was carried out on each surface varying E_S. A diffusion-controlled positive feedback was obtained in all cases, even at the lowest applied substrate overpotential. In fact, a behavior close to the pure diffusion-controlled positive feedback was observed even after a second PEI adsorption. Fig. 5C shows the SECM images of Au/MPS/PEI-NP and Au/MPS/PEI-NP/PEI-dsDNA. The presence of NP in the first bilayer increases the feedback normalized current from ~0.8 at Au/MPS/PEI (Fig. 4) to ~1.15 at Au/MPS/PEI-NP. The comparison between the contour images of Au/MPS/PEI-NP/PEI-dsDNA and Au/MPS/PEI-dsDNA (Fig. 5C plots a and b respectively), clearly evidences that the adsorption of NP

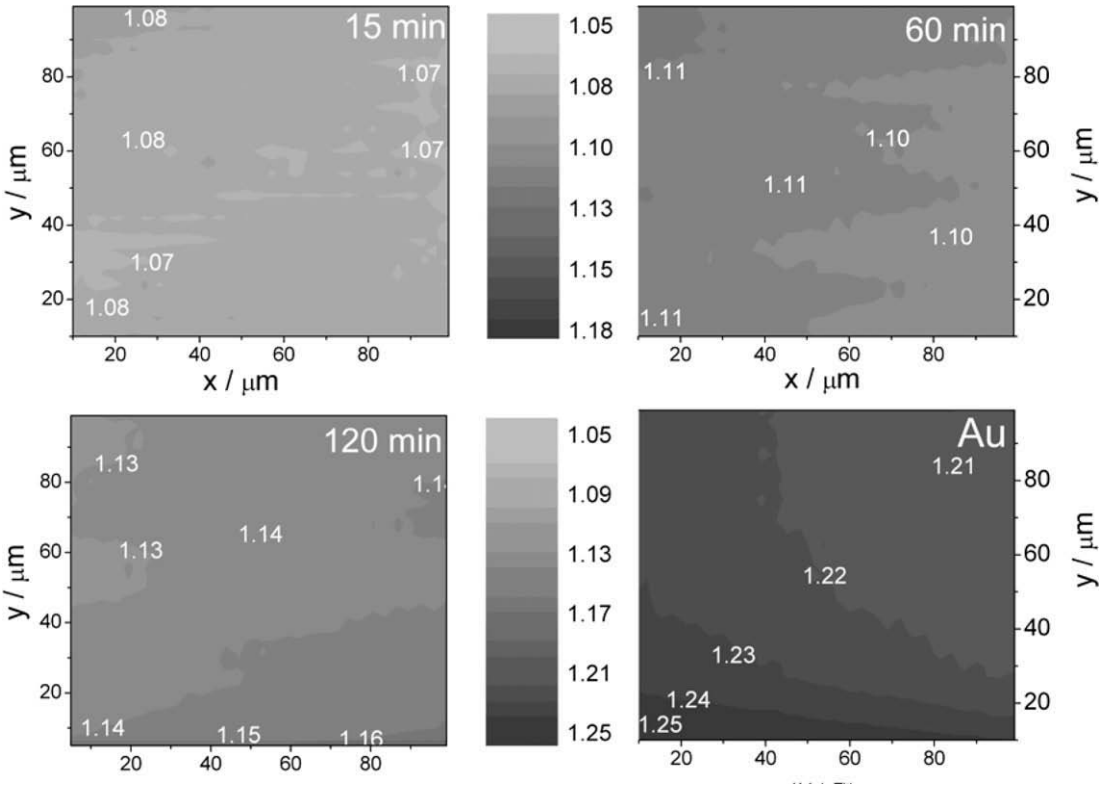

Fig. 6. SECM contour images of Au and Au/MPS/PEI-NP with 15, 60 and 120 min of NP adsorption time. Numbers on the images correspond to normalized current values. Experimental conditions as Fig. 4.

facilitates the electron transfer process of FcOH at the modified surface, since higher feedback currents are obtained when NP are immobilized as a sub-layer of PEI-dsDNA. These results are consistent with those presented in Table 1, where by cyclic voltammetry a decrease in ΔE_p value is observed after the adsorption of NP at the top of PEI. The effect is also detected with the negatively charged FcCOOH, indicating that the increase in the electrochemical response is not consequence of PEI neutralization which should produce a diminution of the electrostatic repulsion, since such effect is not observed after the adsorption of dsDNA.

Several studies have reported that the electrode activity is restored after depositing NP on alkanedithiols [14] or polymers layer [33]. These works indicate that redox reaction can occur at NP surfaces and that NP can act as "electron relays" between the electrolyte solution and the underlying electrode [34]. The effects in the electrochemical responses (e.g., peak height, width, or separation in cyclic voltammograms) are depending on NP size, interparticle spacing, and packing density. To evaluate this point, we analyze the variation of the electrochemical response as function of NPs adsorption time. Fig. 6 shows SECM contour images of Au/MPS/PEI-NP with 15, 60 and 120 min of NP adsorption in comparison with Au. An increase in the feedback current is observed as the NP adsorption time increases. The adsorption of more NP produces an improvement in electrochemical reversibility of redox mediators at the modified electrode and consequently an increased feedback current. At this NP-modified electrodes, the electron communication process could involve two steps: (i) electron transfer between the redox couple and the tethered NP, (ii) electron tunneling through the polymer and thiol layer, between NP and the underlying electrode. The results indicate that, once the nanoparticles adsorption occurs, the number of routes for tunneling changes and, accordingly, the apparent electron transfer rate is modified.

4. Conclusions

Self-assembled multilayers of PEI-dsDNA and PEI-NP were efficiently adsorbed on MPS modified gold electrode. The electron transfer kinetics for the redox probes at different modified surfaces was evaluated from SECM experiments. The k^0 values were highly dependent on the external layer of the self-assembled structure as well as on the mediators charge. Independently of the mediator employed, the adsorption of gold nanoparticles increases the apparent k^0 values that allow obtaining a conductive behavior like bare gold electrodes. The presence of NP also produces an increment in the feedback response including electrodes with PEI-NP as a sub-layer. These results suggest that the development of recognition platforms integrating dsDNA and NP could be an attractive approach to enhance the response of electrochemical biosensors based on the use of DNA as recognition element.

Acknowledgements

The authors thank FONDECYT (Chile) for research grant N^0 1080526 CONICET, SECyT-UNC, Banco Santander Río and ANPCyT (Argentina) for the financial support. The authors also thank to Prof. J. C. Sturm for his help in the microelectrodes manufacture.

References

[1] K. Ariga, J.P. Hill, Q. Ji, Phys. Chem. Chem. Phys. 9 (2007) 231.
[2] G. Decher, in: G. Decher, J.B. Schlenoff (Eds.), Multilayers Thin Films. Sequential Assembly of Nanocomposite Materials, Wiley-VCH, Federal Republic of Germany, 2003 (Chapter 1).
[3] N.F. Ferreyra, L. Coche-Guérente, J. Fatisson, M. Lopez Teijelo, P. Labbé, Chem. Commun. (2003) 2056.
[4] S. Bharathi, M. Nogami, S. Ikeda, Langmuir 17 (2001) 1.
[5] F. Westerlund, T. Bjørnholm, Curr. Opin. Colloid Interface Sci. 14 (2009) 126.
[6] Z. Chang, M. Chen, H. Fan, K. Zhao, Sh. Zhuang, P. He, Y. Fang, Electrochim. Acta 53 (2008) 2939.
[7] W.S. Roberts, D.J. Lonsdale, J. Griffiths, S.P.J. Higson, Biosens. Bioelectron. 23 (2007) 301.
[8] C. Cannes, F. Kanoufi, A.J. Bard, J. Electroanal. Chem. 547 (2003) 83.
[9] G. Wittstock, M. Burchardt, S.E. Pust, Y. Shen, Ch. Zhao, Angew. Chem. Int. Ed. 46 (2007) 1584.
[10] X. Lu, Q. Wang, X. Liu, Anal. Chim. Acta 601 (2007) 10.
[11] B. Liu, A.J. Bard, Ch.Z. Li, H.B. Kraatz, J. Phys. Chem. B 109 (2005) 5193.
[12] S. Bollo, C. Yañez, J. Sturn, L. Nuñez-Vergara, J.A. Squella, Langmuir 19 (2003) 3365.
[13] J. Zhang, R.M. Lahtinen, K. Kontturi, P.R. Unwin, D.J. Schiffrin, Chem. Commun. (2001) 1818.
[14] A. Zabet-Khosousi, Al-Amin Dirán, Chem. Rev. 108 (2008) 4072.
[15] P. Ahonen, V. Ruiz, K. Kontturi, P. Liljeroth, B.M. Quinn, J. Phys. Chem. C 112 (2008) 2724.
[16] V. Ruiz V, P. Liljeroth, B.M. Quinn BM, K. Kontturi, Nano Lett. 3 (10) (2003) 1459.
[17] B.M. Quinn, I. Prieto, S.K. Haram, A.J. Bard, J. Phys. Chem. B 105 (2001) 7474.
[18] A. Escosura-Muñiz, A. Ambrosi, A. Merkoçi, Trends Anal. Chem. 27 (2008) 568.
[19] X. Xiao, Y. Fan, F.R.F. Zhou, A.J. Bard, J. Am. Chem. Soc 130 (2008) 16669.
[20] X. Xiao, Sh. Pan, J.S. Jang, A.J. Bard, J. Phys. Chem. C 113 (2009) 14978.
[21] J. Bard, F.F. Fan, J. Kwak, L. Ovadia, Anal. Chem. 61 (1989) 132.
[22] D.O. Wipf, A.J. Bard, J. Electrochem. Soc. 138 (1991) 469.
[23] S. Bollo, Scanning electrochemical microscopy: basic aspects and applications to electroanalytical sciences, in: J.A. Squella, S. Bollo (Eds.), Electroanalytical Aspects of Biological Significant Compounds, Trandsworld Research Network, Kerala, India, 2006 (Chapter 6).
[24] Allen J. Bard, M.V. Mirkin, P.R. Unwin, D.O. Wipf, J. Phys. Chem. 96 (1992) 1861.
[25] Ch. Mokrani, J. Fatisson, L. Guérente, P. Labbé, Langmuir 21 (2005) 4400.
[26] S. Bollo, S. Finger, J.C. Sturm, L.J. Núñez-Vergara, J.A. Squella, Electrochim. Acta 52 (2007) 4892.
[27] A.J. Bard, M.V. Mirkin, in: J. Bard, M.V. Mirkin (Eds.), Scanning Electrochemical Microscopy, AMarcel Dekker, Inc., New York, 2001.
[28] M.P. Longinottia, H.R. Cort, Electrochemistry Communications 9 (7) (2007) 1444.
[29] J. Velmurugan, P. Sun, M.V. Mirkin, J. Phys. Chem. C 113 (2009) 459.
[30] J.S. Rossier, Ch. Vollet, A. Carnal, G. Lagger, V. Gobry, H.H. Girault, Philippe Michel, Frédéric Reymond, Lab Chip 2 (2002) 145.
[31] C. Amatore, J.M. Savéant, D. Tessier, J. Electroanal. Chem. 147 (1983) 39.
[32] G.B. Sukhorukv, H. Mohwald, G. Decher, Y.M. Lvov, Thin Solid Films 284/285 (1996) 220.
[33] J.J. Kakkassery, J.P. Abid, M. Carrara, D.J. Fermín, Faraday Dis. 125 (2004) 157.
[34] K.R. Brown, A.P. Fox, M.J. Natan, J. Am. Chem. Soc. 118 (1996) 1154.